Published in final edited form as:
Clin Cancer Res. 2012 September 15; 18(18): 5031–5042. doi:10.1158/1078-0432.CCR-12-0453.

Apricoxib, a Novel Inhibitor of COX-2, Markedly Improves Standard Therapy Response in Molecularly Defined Models of Pancreatic Cancer

Amanda Kirane[1], **Jason E. Toombs**[1], **Katherine Ostapoff**[1], **Juliet G. Carbon**[1], **Sara Zaknoen**[2], **Jordan Braunfeld**[1], **Roderich E. Schwarz**[1], **Francis J. Burrows**[2], and **Rolf A. Brekken**[1]

[1]Division of Surgical Oncology, Department of Surgery, The Hamon Center for Therapeutic Oncology Research, University of Texas Southwestern Medical Center, Dallas, Texas

[2]Tragara Pharmaceuticals, Inc., San Diego, California

Abstract

Purpose—COX-2 is expressed highly in pancreatic cancer and implicated in tumor progression. COX-2 inhibition can reduce tumor growth and augment therapy. The precise function of COX-2 in tumors remains poorly understood, but it is implicated in tumor angiogenesis, evasion of apoptosis, and induction of epithelial-to-mesenchymal transition (EMT). Current therapeutic regimens for pancreatic cancer are minimally effective, highlighting the need for novel treatment strategies. Here, we report that apricoxib, a novel COX-2 inhibitor in phase II clinical trials, significantly enhances the efficacy of gemcitabine/ erlotinib in preclinical models of pancreatic cancer.

Experimental Design—Human pancreatic cell lines were evaluated *in vitro* and *in vivo* for response to apricoxib ± standard-of-care therapy (gemcitabine + erlotinib). Tumor tissue underwent posttreatment analysis for cell proliferation, viability, and EMT phenotype. Vascular parameters were also determined.

Results—COX-2 inhibition reduced the IC_{50} of gemcitabine ± erlotinib in six pancreatic cancer cell lines tested *in vitro*. Furthermore, apricoxib increased the antitumor efficacy of standard combination therapy in several orthotopic xenograft models. *In vivo* apricoxib combination therapy was only effective at reducing tumor growth and metastasis in tumors with elevated COX-2 activity. In each model examined, treatment with apricoxib resulted in vascular

Corresponding Author: Rolf A. Brekken, Hamon Center for Therapeutic Oncology Research, UT Southwestern Medical Center, 6000 Harry Hines Blvd, Dallas, TX 75390. Phone: 214-648-5151; Fax: 214-648-4940; rolf.brekken@utsouthwestern.edu.

Disclosure of Potential Conflicts of Interest

R.A. Brekken has received a commercial research grant from Tragara Pharmaceuticals, Inc. F. J. Burrows and S. Zaknoen are employees of Tragara Pharmaceuticals, Inc. No potential conflicts of interest were disclosed by the other authors.

Authors' Contributions

Conception and design: A. Kirane, F. J. Burrows, R. A. Brekken
Development of methodology: A. Kirane
Acquisition of data (provided animals, acquired and managed patients, provided facilities, etc.): A. Kirane, J. E. Toombs, K. T. Ostapoff, J. G. Carbon
Analysis and interpretation of data (e.g., statistical analysis, biostatistics, computational analysis): A. Kirane, K. T. Ostapoff, J. B. Braunfeld, F. J. Burrows, R. A. Brekken
Writing, review, and/or revision of the manuscript: A. Kirane, S. Zaknoen, R. E. Schwarz, F. J. Burrows, R. A. Brekken
Administrative, technical, or material support (i.e., reporting or organizing data, constructing databases): A. Kirane, R. E. Schwarz, F. J. Burrows
Study supervision: A. Kirane, R. A. Brekken

normalization without a decrease in microvessel density and promotion of an epithelial phenotype by tumor cells regardless of basal COX-2 expression.

Conclusions—Apricoxib robustly reverses EMT and augments standard therapy without reducing microvessel density and warrants further clinical evaluation in patients with pancreatic cancer.

Introduction

The progression of several human cancers, including pancreatic, has been linked to inflammation, which can trigger secretion of growth factors, infiltration of immune cells, and DNA damage by reactive oxygen species leading to tumor cell proliferation and escape from cell death (1). Epidemiologically, chronic use of anti-inflammatory drugs correlates with a reduction in the incidence of certain cancers, including pancreatic cancer (2, 3). Upregulation of cyclooxygenase-2 (COX-2), the rate limiting step in the synthesis of prostaglandins from arachidonic acid, is an early inflammatory response and is regulated by several growth factors and cytokines (4). Elevated COX-2 expression is frequent in many cancers, including pancreatic cancer where it is expressed highly in up to 75% of cases (5). Increased COX-2 in pancreatic tumors correlates with increased invasiveness and shorter overall survival (6–10). The most abundant product of COX-2 in tumors, prostaglandin E_2 (PGE_2), can affect multiple carcinogenic pathways and participate in proliferation, invasion, angiogenesis, chemoresistance, and metastasis (5, 11–14). In the pancreas under normal conditions, only islet cells express COX-2 (10). As pancreatic intraepithelial lesions develop, COX-2 expression is elevated and the use of COX-2 inhibitors can delay the progression of the disease in preclinical KRas-driven mouse models. Indeed, inhibition of COX-2 can reduce tumor growth in several experimental models of pancreatic cancer (15, 16). Importantly, prostaglandins secreted from stromal fibroblasts facilitate tumor cell proliferation and survival even in tumors and cell lines where COX-2 is not expressed by tumor cells, suggesting that COX-2 is an important signaling molecule in the tumor microenvironment (17). Collectively, these findings make COX-2 an attractive target for anticancer therapy.

Despite advances in diagnostics and treatment, the prognosis for inoperable pancreatic cancer remains poor, largely because of local invasion and metastatic progression at early stages (18). The current standard-of-care for pancreatic cancer is gemcitabine but it affords minimal survival benefit to patients (19). Addition of the COX-2 inhibitor celecoxib to gemcitabine-containing regimens have yielded mixed results; indeed, strategies to augment gemcitabine activity have largely failed to improve overall survival in phase III clinical studies, excepting combination with erlotinib, an inhibitor of EGF receptor (EGFR). However, while statistically significant, erlotinib-based improvement remains modest (20, 21). Rationale exists for the combined targeting of EGFR and COX-2 as significant overlap and interaction occur between these pathways. PGE_2 can transactivate EGFR, which can subsequently increase expression of COX-2. In addition, PGE_2, via promotion of epithelial-to-mesenchymal transition (EMT), can increase resistance to EGFR inhibitors (22). Furthermore, short circuiting both pathways simultaneously can have synergistic effects in preclinical cancer models (23–25).

The mechanistic basis of COX-2 inhibitor therapy in pancreatic cancer remains ill-defined, although in the HT29 model of colorectal cancer reversion of the EMT phenotype has been reported to be a key mechanism of action (26). Apricoxib is a novel, selective COX-2 inhibitor currently in phase II studies for NSCLC and pancreatic cancer. Apricoxib has showed significant antitumor effects in xenograft models of lung and colorectal cancer and seems more potent than previous COX-2 inhibitors (23, 27, 28). In this study, we characterized the baseline expression and activity of EGFR and COX-2 in commonly

employed pancreatic cancer cell lines as well as functional responses to inhibition of each pathway. *In vivo* studies with COX-2–positive and -negative cell lines showed that addition of apricoxib enhanced the antitumor efficacy of gemcitabine and erlotinib in COX-2-dependent models. We present evidence that apricoxib adds significantly to the treatment effect of standard therapy in COX-2 expressing cell lines and also promotes vascular stabilization while reversing EMT regardless of the COX-2 status of the primary tumor.

Materials and Methods

Cell lines

Human pancreatic cancer cell lines AsPC-1, Su.86.86, HPAF-II, PL45, and CFPAC-1 were obtained from ATCC (Manassas, VA); Colo357 was obtained from MD Anderson Cancer Center. AsPC-1 and PL45 were grown in DMEM, CFPAC-1 in IMDM, Colo357 and HPAF-II in MEM, and Su.86.86 in RPMI (Fisher). All cell lines were grown in a humidified atmosphere with 5% CO_2, at 37°C, and have been DNA fingerprinted for provenance using the Power-Plex 1.2 kit (Promega) and confirmed to be the same as the DNA fingerprint library maintained by ATCC and confirmed to be free of mycoplasma by the e-Myco kit (Boca Scientific).

Baseline expression status

For Western blot analysis, cell lysates were produced using MPER (Pierce) with added protease and phosphatase inhibitors (Pierce) and protein concentration was determined by BCA assay (Pierce). Immunodetection was conducted by electrophoretic transfer of SDS-PAGE separated proteins to PVDF membranes. Antibodies used for Western blot analysis included EGFR (Upstate), Tyr 1069 phospho-EGFR, and Cox-2 (Santa Cruz).

For PCR analysis, RNA was prepared using TRIzol (Invitrogen) per manufacturer instructions and concentration was determined by spectrophotometry. The cDNA used for subsequent for PCR was made using iScript (Bio-Rad Laboratories) and Choice DNA Taq polymerase (Denville Scientific). The expression of COX-2 and EGFR was analyzed by quantitative real-time PCR using β-actin as an internal reference gene. Each reaction was conducted in triplicate with RNA harvested from 3 independent cell cultures. The comparative Ct method was used to compute relative expression values (29).

In vitro cytotoxicity and drug response assay

MTS assays were conducted in 96-well plates; cells were plated on day 0 and drug was added on day 1 in 4-fold dilutions. Drugs were evaluated as single agents with maximum concentration of 2,000 nmol/L for gemcitabine and 400 μmol/L for erlotinib and apricoxib. For combination studies gemcitabine was added with a fixed concentration of 1 μmol/L erlotinib, 0.1 μmol/L apricoxib, or 1 μmol/L apricoxib, and triple combination with 1 μmol/L erlotinib and 1 μmol/L apricoxib. Relative cell number was determined by adding MTS (Promega; final concentration 333 μg/mL), incubating for 1 to 3 hours at 37°C, and reading absorbance. Drug sensitivity curves and IC_{50}s were calculated using in-house software (30).

Phospho-EGFR ELISA (R&D Systems) was conducted after incubating cells overnight in a 96-well plate, serum starving for 4 hours, and stimulating for 15 minutes with 10 ng/mL EGF. The plate was processed per manufacturer instructions. PGE_2 ELISA (Cayman) was used to evaluate PGE_2 levels in conditioned media. Cells were plated in 24-well plates overnight and incubated for 24 hours with increasing concentrations of apricoxib in low serum medium. Assays were conducted in triplicate and were carried out minimum of 3 times.

Animal studies

All animals were housed in a pathogen-free facility with 24-hour access to food and water. Experiments were approved by, and conducted in accordance with, the IACUC at UT Southwestern (Dallas, TX). Four- to 6-week-old female NOD/SCID mice were obtained from a campus supplier. A total of 1×10^6 AsPc-1, Colo357, and HPAF-II cells were injected orthotopically as described (30) and tumor growth monitored by ultrasound. Mice with established tumors were randomized to receive either gemcitabine 25 mg/kg twice weekly plus erlotinib 100 μg daily (standard-of-care), or standard-of-care plus 10 or 30 mg/kg apricoxib daily by oral gavage. Mice bearing Colo357 and AsPc-1 tumors received 3 weeks of therapy prior to sacrifice. Animals bearing HPAF-II tumors were divided into an early sacrifice at 3 weeks and a late sacrifice at 7 weeks of therapy. Primary tumor burden was established by weighing pancreas and tumor en bloc. Metastatic incidence was determined by visual inspection of the liver and abdominal cavity as well as by quantitation of H&E liver sections. Tissues were fixed in 10% formalin or snap-frozen in liquid nitrogen for further studies.

Histology and tissue analysis

Formalin-fixed tissues were embedded in paraffin and cut in 10-μm sections. Sections were evaluated by H&E and immunohistochemical analysis using antibodies CD31 (Dianova), NG2 (Millipore), vimentin (Phosphosolutions), endomucin, Zeb1, E-cadherin, PCNA (Santa Cruz), phosphohistone H3 (Upstate), TUNEL (Promega), cleaved caspase-3 (Cell Signaling), VEGF, and COX-2 (Abcam). Negative controls included omission of primary antibody and immunofluorescent evaluation was conducted as described (31). Human and mouse VEGF levels in plasma and tumor lysates were determined by ELISA (R&D Systems) per manufacturer instructions.

Statistics

Data were analyzed using GraphPad software (GraphPad Prism version 4.00 for Windows; GraphPad Software; www.graphpad.com). Results are expressed as mean ± SEM. Data were analyzed by *t* test or ANOVA and results are considered significant at $P < 0.05$.

Results

Human pancreatic cancer cell lines vary in expression of COX-2 and EGFR and show differential response to inhibition

Five human pancreatic cancer cell lines were screened for baseline expression of COX-2 and EGFR by qPCR. All cell lines expressed detectable levels of mRNA for EGFR and COX-2. There was generally close accordance between message and protein, except COX-2 levels in AsPC-1 cells that were detectable (albeit barely) by qPCR (Fig. 1A) but not at the protein level (Fig. 1B). Colo357 cells showed moderate-to-high expression of COX-2 at the mRNA and protein level (Fig. 1A and B). PL45, HPAF-II, and CFPAC-1 cells exhibited low-to-moderate expression of COX-2 at the mRNA and protein level (Fig. 1A and B). EGFR expression was detectable in all cell lines by qPCR. The majority of cells displayed low-to-moderate expression with the exception of AsPC-1, which showed relatively high expression (Fig. 1A). Expression of EGFR at the protein level was assessed by Western blot and confirmed robust expression of EGFR in AsPC-1 cells. However, it was notable that phosphorylated EGFR (p-EGFR) was weak or not detected in the majority of cell lines under basal conditions. In contrast, there was a strong p-EGFR signal in Colo357 cells (Fig. 1B). The efficacy of erlotinib inhibition of p-EGFR after stimulation with EGF in each cell line was determined by ELISA (Fig. 1C). AsPC-1 and HPAF-II cells were most sensitive with IC_{50}s of 0.1 and 0.2 μmol/L, respectively. All cells showed an IC_{50} below the

pharmacologic range (2.2 μmol/L) with the exception of PL45 cells, which were resistant to erlotinib at maximum dose (500 μmol/L; Fig. 1C). To determine the effect of apricoxib, conditioned media of cells incubated for 24 hours with apricoxib was collected and PGE_2 levels determined. Baseline levels of PGE_2 production by AsPC-1 and PL45 cells was minimal at <10 pg/mL (below detectable range) and remained unchanged by apricoxib treatment (AsPC-1 shown; Fig. 1D). Apricoxib effectively prevented PGE_2 production by Colo357 and HPAF-II cells with IC_{50}s within the pharmacologic range (0.5–2 μmol/L, Colo357, shown in Fig. 1D). CFPAC-1 displayed a dose-dependent reduction but did not achieve an IC_{50} within the tested range (max 1 μmol/L, data not shown). From this we concluded that all cell lines except PL45 show inhibition of EGFR activity *in vitro* at pharmacologically relevant concentrations of drug; however, although most cell lines express COX-2, this did not directly correlate to level of PGE_2 production. For cell lines with detectable PGE_2 expression, apricoxib inhibited its production at nanomolar concentrations *in vitro*.

Erlotinib and apricoxib combination therapy augments efficacy of gemcitabine *in vitro*

MTS assays were used to evaluate the antiproliferative effect of each drug as a single agent and in combination. As shown in Table 1, the IC_{50} for erlotinib and apricoxib as single agents was above pharmacologic range for all cell lines. AsPC-1, Su.86.86, and HPAF-II showed the least sensitivity to apricoxib as a single agent, with IC_{50} values of 70 to 80 μmol/L. Cell lines insensitive to gemcitabine (IC_{50}not achieved with maximum dose 2000 nmol/L) included AsPC-1, HPAF-II, and Su.86.86. Highly gemcitabine sensitive lines included PL45 and CFPAC-1. Colo357 showed an intermediate antiproliferative response with an IC_{50} of 150 μmol/L. Addition of 0.1 μmol/L apricoxib did not significantly alter response to gemcitabine in any cell line other than Colo357, which showed 1.3-fold reduction in gemcitabine IC_{50}. Apricoxib at 1 μmol/L enhanced the response of AsPC-1, HPAF-II, and Colo357 to gemcitabine but had little effect on gemcitabine activity in the remaining lines. Erlotinib augmented response to gemcitabine in all lines evaluated. Triple combination of gemcitabine, 1 μmol/L erlotinib, and 1 μmol/L apricoxib showed measurable reduction of gemcitabine IC_{50} in all cell lines (Table 1); sensitization was particularly marked in HPAF-II cells, where the gemcitabine IC_{50} was reduced by over 3 orders of magnitude by the combination of apricoxib and erlotinib. Colo357 and HPAF-II, as lines expressing COX-2 and showing sensitization to gemcitabine with COX-2 inhibition, were selected for further *in vivo* studies in addition to AsPC-1, a COX-2–negative cell line.

Inhibition of COX-2 significantly reduces primary tumor growth *in vivo* and metastatic incidence in cell lines with high COX-2 expression

From the *in vitro* data we selected a COX-2–negative cell line, AsPC-1, and 2 COX-2 positive cell lines, one with minimal erlotinib response, Colo357, and a highly erlotinib sensitive line, HPAF-II for *in vivo* studies. Mice began therapy 10 to 14 days postorthotopic tumor cell injection. Therapy consisted of control (vehicle alone), standard therapy, that is 25 mg/kg gemcitabine + 100 μg erlotinib (G +E), or G + E + apricoxib at 10 or 30 mg/kg. AsPC-1 and Colo357 tumor bearing mice were sacrificed after 3 weeks of therapy. Tumor and pancreas were dissected en bloc to determine tumor weight. Metastatic burden was initially surveyed by inspection of the abdominal cavity, diaphragm, and liver and later quantified by H&E staining of the left lobe of the liver. For AsPC-1 tumors, addition of apricoxib resulted in a significant decrease in primary tumor weight compared with control treated animals ($P < 0.05$, 2-tailed *t* test, Mann-Whitney); however, the effect was equivalent to the standard-of-care, showing that the antitumor activity was because of gemcitabine and erlotinib in this model (Fig. 2A). Metastatic burden in AsPC-1 bearing mice was highly variable with no significant differences between groups (Fig. 2B). Mice bearing Colo357 tumors showed a significant reduction in primary tumor size with the standard-of-care alone

compared with saline ($P < 0.05$; ANOVA) and the effect was further enhanced by apricoxib treatment ($P < 0.05$; ANOVA). Metastases in animals bearing Colo357 were virtually eliminated in apricoxib-treated groups, with 10 mg/kg showing greatest response ($P < 0.005$ compared with G + E, Dunn MCT; Fig. 2B). Mice bearing HPAF-II tumors received therapy for 3 weeks, at which point saline controls were moribund and required sacrifice. HPAF-II tumors were highly sensitive to erlotinib treatment and at this time all treatment groups had virtually no tumor growth, thus it was elected to sacrifice only 3 animals/group for comparison to control and allow remaining mice to continue on therapy. There were no differences in tumor burden among treatment groups at the 3-week time point with all final weights being equivalent to normal pancreas weight. The remaining animals continued on therapy for an additional 4 weeks, at which point apricoxib-treated animals showed superior tumor control rate compared with G + E ($P < 0.001$; ANOVA). Metastases in the HPAF-II model were suppressed significantly in all treatment groups compared with control animals, but again apricoxib enhanced the activity of G +E, abolishing metastatic spread altogether (Fig. 2A and B).

Given the small primary tumor burden of HPAF-II, which largely consisted of normal pancreas, only Colo357 and AsPC-1 tumors were used for further evaluation. Paraffin-embedded tumor sections were used to analyze COX-2 expression by immunofluorescence.

COX-2 expression can be induced *in vivo* and *in vitro* upon EMT in a COX-2–negative cell line

Notably, although AsPC-1 cells did not express measurable levels of COX-2 *in vitro*, untreated AsPC-1 xenografts stained positive for COX-2, although to a far lesser extent than Colo357 tumors. Interaction of EGFR and COX-2 signaling (24) is supported by a clear reduction in COX-2 expression by G + E treatment, although this value was not statistically significant in either group. Apricoxib treatment virtually eliminated COX-2 expression in tumors from both cell lines. PGE_2 is rapidly metabolized in plasma and therefore difficult to assess *in vivo*. However, PGE_2 stimulates COX-2 expression, forming a positive feedback loop, so reduction in overall COX-2 levels shows that apricoxib effectively inhibits PGE_2 production *in vivo* (32, 33). In COX-2 expressing tumors, this resulted in increased efficacy of standard therapy (Fig. 2A and B). It has been reported that a COX-2 nonexpressing cell line can upregulate COX-2 under conditions of stress. To recapitulate *in vivo* changes resulting from tumor–host interactions, PGE_2 production was evaluated after forced EMT (26). In Colo357, PGE_2 production was not significantly different between normal and EMT conditions at baseline. At 24 hours after a single dose of apricoxib (0.5 μmol/L), representing the lowest range of *in vivo* levels (26), PGE_2 levels had decreased by 50% for both conditions. AsPC-1 cells, which produce no measurable amount of PGE_2 at baseline, showed a significant increase in PGE_2 levels after induction of EMT. In contrast to Colo357, this was not affected by apricoxib (Fig. 2E).

Inhibition of COX-2 attenuates VEGF and promotes vascular normalization *in vivo*

COX-2 expression correlates with VEGF levels in patient tumor samples and COX-2 inhibition can modulate VEGF production (27, 34). VEGF levels in plasma and tumor samples collected from mice tumor-bearing mice were measured by ELISA. In AsPC-1 tumor-bearing mice, plasma VEGF levels were decreased in all treatment groups, but these differences were not significantly different from control-treated animals. In Colo357 tumor-bearing mice, VEGF levels were unaffected by G + E treatment but addition of apricoxib resulted in depletion of human VEGF from plasma samples (Fig. 3A). Interestingly, these changes did not correlate with intratumoral levels of human VEGF. In fact, the lowest levels of tumor-associated VEGF were found in G + E-treated animals (NS for AsPC-1 tumors, $P < .005$ in Colo357 tumors; Fig. 3B).

To assess the ultimate effect of COX-2 inhibition on angiogenesis, tumor microvessel density was evaluated by immunofluorescence for endomucin and CD31 (CD31 shown; Fig. 3C and D). Vessel density was decreased moderately by G + E alone (NS for Colo357 but trending downward, $P < 0.05$ for AsPC-1); however, addition of apricoxib to the treatment regimen did not significantly alter the effect of G + E on vessel density (Fig. 3C). To determine if therapy affected pericyte–endothelial cell interaction, NG2, a pericyte marker, was colocalized with endomucin or CD31 to assess pericyte coverage of vessels. Pericyte coverage index (%NG2 positive vessels) increased significantly in apricoxib-treated AsPC-1 and Colo357 tumors ($P < 0.001$ AsPC-1, <0.05 Colo357, ANOVA; Fig. 3C, D). In summary, COX-2 inhibition did alter plasma levels of VEGF but this did not translate to a change in levels of tumor-associated VEGF or neovascularization, instead COX-2 inhibition promoted vascular stabilization, which may improve drug delivery as well as contribute to the reduction of metastases (35).

Inhibition of COX-2 reduces proliferation and increases apoptosis

Inhibition of COX-2 activity with apricoxib enhanced the antitumor effect of G + E. To determine if this was because of changes in cell proliferation or survival, we evaluated markers of apoptosis and cell proliferation in AsPC-1 and Colo357 tumors. The level of apoptosis in tumors from control and treated animals was determined by TUNEL (Fig. 4A and B). Apricoxib significantly increased the number of apoptotic cells in AsPC-1 and Colo357 tumors. The increase in TUNEL was most evident at the 10 mg/kg dose (Fig. 4A), but animals treated with 30 mg/kg of apricoxib showed the highest levels of cleaved caspase-3 levels (data not shown). In AsPC-1 tumors, proliferative markers (phosphohistone H3 and PCNA) were unchanged (data not shown and Fig. 4C). By contrast, apricoxib strongly enhanced the modest anti-proliferative effect of G + E in Colo357 tumors, especially at the 30 mg/kg dose ($P < 0.01$; Fig. 4C and D). To substantiate the effect of apricoxib on the efficacy of standard therapy, we evaluated γH2AX levels, which have been shown to mark gemcitabine-induced stalled replication forks (36). yH2AX expression was evaluated by immunofluorescence in Colo357 tumor sections and found to be significantly increased in apricoxib treated tumors compared with either control or G + E treatment alone ($P < 0.05$; Fig. 4E).

COX-2 inhibition reverses EMT

We have recently found that apricoxib reverses EMT in HT29 xenografts (26); thus, we assessed tumor sections in this study for epithelial (E-cadherin) and mesenchymal (vimentin, and Zeb-1) markers by immunofluorescence. In Colo357 tumors, vimentin and Zeb1 expression decreased in a dose-dependent fashion in apricoxib-treated animals compared with control and G +E groups, although changes in vimentin expression did not reach statistical significance ($P < 0.05$ vs. control, G + E for Zeb1; Fig. 5A). Conversely, E-cadherin was strongly induced by apricoxib treatment ($P < 0.001$ vs. control, G + E; Fig. 5A). Representative double-stained images are shown for vimentin and E-cadherin in Colo357 tumors (Fig. 5B). Untreated Colo357 tumors showed a mesenchymal phenotype with strong vimentin positive staining and negligible E-Cadherin expression. By comparison, Colo357 cells *in vitro* show an epithelial phenotype that seems preserved (or reacquired) after apricoxib treatment (Fig. 5C). Treatment of cells in culture with G +E alone actually increased Zeb1 expression, but combination with apricoxib reversed this effect and dramatically upregulated E-Cadherin expression (Fig. 5C).

Inhibition of COX-2 resulted in a shift toward a more epithelial phenotype regardless of baseline COX-2 status of the tumor; although this effect was more dramatic in high COX-2 expressing Colo357 tumors and correlated with the overall reduction of metastatic incidence. AsPC-1 cells, which increased COX-2 expression *in vivo* and following EMT *in*

vitro (Fig. 2E), show this shift toward epithelial phenotype by apricoxib treatment with decreased vimentin and Zeb1 and dramatically increased E-Cadherin expression (Fig. 5D). *In vitro*, Zeb1 expression by AsPC-1 cells is unchanged after G + E or combination with apricoxib. As these cells have undetectable COX-2 expression and PGE_2 production under normal culture conditions, EMT was induced in these cells to recapitulate *in vivo* changes. Following EMT, apricoxib treatment either in combination with G + E or as a single agent at 1 μmol/L significantly diminished Zeb1 expression, this shift did not occur with G + E alone, suggesting that COX-2 is intimately involved with the occurrence of EMT and that transformed cells that undergo EMT show increased sensitivity to apricoxib.

Discussion

Resistance to chemotherapy remains a major challenge in the treatment of pancreatic cancer, combination strategies to augment gemcitabine failed to show improved overall survival in phase III clinical trials before addition of erlotinib (20). Early results of small phase II studies combining the COX-2 inhibitor celecoxib with gemcitabine or gemcitabine plus irinotecan showed promise with prolonged survival compared with the historic average survival of 6 months for gemcitabine (23). Apricoxib is currently in phase II clinical trials in NSCLC and pancreatic cancer. Our studies aimed to determine the antitumor activity of apricoxib in molecularly defined preclinical pancreatic cancer models with the hope of identifying subsets of pancreatic cancer patients who would benefit from the addition of COX-2 inhibition to current therapy.

In vitro, we determined the mRNA and protein expression of EGFR and COX-2 in cancer cell lines and measured how these targets contribute to cellular response to gemcitabine. We found in all cell lines that concentrations of apricoxib required to exert direct antitumor activity far exceeded those needed to eliminate PGE_2 production (0.5–2 μmol/L). However, apricoxib at pharmacologically achievable concentrations sensitized cells to standard therapy. This suggests that antitumor effects of COX-2 inhibition in these models *in vivo* resulted primarily from sensitization to gemcitabine/erlotinib therapy or modification of tumor–host interactions as opposed to direct antitumor cell effects, although it is possible that COX-2-dependent lines would have responded under anchorage-independent growth conditions (26). This is also supported by the increased production of PGE_2 *in vitro* by AsPC-1 following forced EMT corresponding to increased COX-2 expression by cells *in vivo* which have adopted an increasingly mesenchymal phenotype.

In vivo, in mice bearing tumors derived from AsPC-1, a COX-2 low-expressing cell line, addition of apricoxib to standard therapy did not improve antitumor activity nor dramatically effect cell proliferation as measured by PCNA expression. By contrast, in cell lines that express moderate to high levels of COX-2 and produce high levels of PGE_2, significantly increased efficacy was achieved by the addition of apricoxib. These results suggest that clinical studies should consider COX-2 activity, not simply expression, when evaluating apricoxib or other COX-2 inhibitors in cancer patients. Assaying the level of PGEM, a PGE_2 metabolite, is a potential strategy for patient stratification.

COX-2 and PGE_2 are strongly linked to angiogenesis via promotion of VEGF and bFGF production stimulating growth, migration, and survival of endothelial cells (27, 34). Reciprocally, these factors form a positive feedback loop amplifying the production of COX-2. In our studies, apricoxib did modulate VEGF levels in plasma but this did not result in a reduction in microvessel density. In all tumor groups, VEGF levels were observed to be lowest in tumors that received standard (G + E) therapy. High expression of COX-2 corresponds to high VEGF levels in tumor specimens; however, studies have reported that although VEGF production is reduced initially by COX-2 inhibition, its production is not

exclusively COX-2 dependent. Recovery and amplification of VEGF levels may occur as a compensatory response to loss of COX-2 activity and levels of VEGF continue to increase with higher doses of COX-2 inhibitors (15, 37, 38). This may provide a plausible explanation for the paradoxical dose–response in our models, as well as other preclinical studies. Furthermore, these data might also help explain the failure of COX-2 inhibitors to show significant improvement in clinical studies that previously employed doses twice that used for analgesic and anti-inflammatory effect (39, 40). Reciprocally, mechanisms of anti-VEGF resistance may involve induction of other pro-angiogenic cytokines, such as IL-1β and IL-8 that are associated with increased COX-2 production in the tumor microenvironment. This collateral pathway may explain why COX-2 inhibition alone failed to be significantly antiangiogenic in this model.

Microvessel density was reduced in all therapy groups receiving standard therapy and was unchanged by the addition of apricoxib. The decrease in microvessel density by treatment with gemcitabine has been reported previously (41) and may be a result of the dosing schedule employed. However, apricoxib treatment resulted in increased pericyte coverage of blood vessels. Pericyte attachment is critical for stabilizing vascular structures (35). Absent or loose pericyte attachment results from imbalanced angiogenic signaling in the tumor leading to dysfunctional vessels that are hallmarked by hyperpermeability. These vessels display abnormal blood flow than can increase tumor hypoxia, reduce delivery of chemotherapy and facilitate extravasation and hematogenous spread of metastatic cells (35). COX-2 inhibition impeded this process, suggesting that COX-2 participates in vascular remodeling in the tumor microenvironment.

The COX-2 product PGE_2 can impact tumor progression and cancer cell proliferation by activating the Ras-MAPK signaling cascade, which subsequently increases expression of PGE_2 synthase, forming a positive feedback loop (42, 43). In addition, exogenous PGE_2 can stimulate proliferation of COX-2–negative cells *in vitro* (17). PGE_2 can mediate cell survival by inducing expression of antiapoptotic proteins such as Bcl-2 and increasing NF-κB transcriptional activity (44). Chemotherapy can increase COX-2 protein expression and PGE_2 production, driving tumor cell survival and resistance to therapy. In this study, proliferative activity *in vivo* was not affected by COX-2 inhibition in AsPC-1 tumors; however, apricoxib significantly reduced proliferation in Colo357 tumors. Apoptosis resulting from COX-2 inhibition, alternatively, was not specific to COX-2 status of the tumor and in each group was most profound in the 10 mg/kg group; indicating that adaptation of AsPC-1 cells *in vivo* can lead to increased dependency on COX-2. γH2AX has been implicated as a marker of gemcitabine specific DNA damage and was found to be significantly elevated in apricoxib treated tumors. This finding correlated with improvement in apoptotic activity and vessel maturity, indicating that improved chemotherapeutic response may be related in part to improved drug delivery.

COX-2 and PGE_2 are implicated in driving EMT (45, 46), which contributes to metastasis and resistance to chemotherapy (47, 48). We found that untreated Colo357 and AsPC-1 tumors displayed a robust EMT phenotype. In contrast, tumor-bearing mice that received apricoxib had a noticeable shift to an epithelial phenotype. These observations suggest that COX-2 inhibition can reverse EMT in pancreatic tumors. PGE_2 directly induces the transcription factor Zeb1 and enhances its binding to the proximal e-box of the E-cadherin promoter, resulting in downregulation of E-cadherin. E-cadherin is essential for intercellular adhesion, such that disruption facilitates migration, invasion, and metastasis (5, 49). Clinical tumor samples have shown an inverse relationship between COX-2 expression/high-grade tumor type and E-cadherin expression (49). Vimentin, a marker of mesenchymal differentiation, is also highly expressed in pancreatic cancers and correlates with poor prognosis (47). Notably, gemcitabine resistance has been linked to vimentin expression in

pancreatic cancer cells (50). *In vitro*, apricoxib dramatically increased E-cadherin expression in Colo357 cells as well as reversed the increased Zeb1 production observed after G + E treatment. Unsurprisingly, no affect was seen in AsPC-1 cells at baseline as they have minimal baseline COX-2 activity. However, the increased COX-2 production with forced EMT greatly sensitized these cells to apricoxib and showed that apricoxib effectively reversed EMT. This suggests that the maintenance of the mesenchymal phenotype in these cells relies in part on the activity of COX-2. *In vivo*, minimal change was seen in the mesenchymal phenotype of Colo357 tumors with standard therapy, although G + E increased Zeb-1 and vimentin in AsPC-1 tumors. Addition of apricoxib significantly shifted AsPC-1 tumors toward a more epithelial phenotype, although it should be noted that AsPC-1 tumors are typically epithelial at baseline. This may explain why these shifts, while present, may not have an overwhelming impact on overall tumor response. Importantly, Colo357 tumors showed a dose-dependent mesenchymal-to-epithelial transition (MET). Although this did not translate into a reduction in metastatic burden for AsPC-1 tumors, the effect was dramatic in Colo357 tumor-bearing mice, implicating COX-2 as important in governing EMT and sensitization to standard therapy in pancreatic cancer.

In summary, our findings show that the clinical COX-2 inhibitor, apricoxib, enhances the efficacy of standard chemotherapy in preclinical models of pancreatic cancer. Inhibition of COX-2-mediated PGE_2 production enhanced the antiproliferative and apoptotic effect of standard therapy in COX-2-dependent tumors and affected the tumor micro-environment by promoting vascular normalization and attenuating EMT. Further clinical evaluation of apricoxib in a molecularly selected patient population is warranted in the development of strategies to improve treatment for pancreatic cancer.

Acknowledgments

The authors thank Surya Vadrevu for technical assistance and Drs. Joan Schiller, David H. Johnson, and John Minna and members of the Brekken laboratory for advice and thoughtful discussion.

Grant Support

This work was supported in part by a sponsored research agreement from Tragara Pharmaceuticals, Inc. and the Effie Marie Cain Scholarship in Angiogenesis Research (to R. A. Brekken) and an institutional training grant from the NCI (T32 CA136515, to A. Kirane).

References

1. Sobolewski C, Cerella C, Dicato M, Ghibelli L, Diederich M. The role of cyclooxygenase-2 in cell proliferation and cell death in human malignancies. Int J Cell Biol. 2010; 2010:215158. [PubMed: 20339581]
2. Harris RE, Beebe-Donk J, Doss H, Burr Doss D. Aspirin, ibuprofen, and other non-steroidal anti-inflammatory drugs in cancer prevention: a critical review of non-selective COX-2 blockade (review). Oncol Rep. 2005; 13:559–83. [PubMed: 15756426]
3. Dannenberg AJ, Subbaramaiah K. Targeting cyclooxygenase-2 in human neoplasia: rationale and promise. Cancer Cell. 2003; 4:431–6. [PubMed: 14706335]
4. Williams CS, Mann M, DuBois RN. The role of cyclooxygenases in inflammation, cancer, and development. Oncogene. 1999; 18:7908–16. [PubMed: 10630643]
5. Dohadwala M, Yang SC, Luo J, Sharma S, Batra RK, Huang M, et al. Cyclooxygenase-2-dependent regulation of E-cadherin: prostaglandin E(2) induces transcriptional repressors ZEB1 and snail in non-small cell lung cancer. Cancer Res. 2006; 66:5338–45. [PubMed: 16707460]
6. Deer EL, Gonzalez-Hernandez J, Coursen JD, Shea JE, Ngatia J, Scaife CL, et al. Phenotype and genotype of pancreatic cancer cell lines. Pancreas. 2010; 39:425–35. [PubMed: 20418756]

7. Hasan S, Satake M, Dawson DW, Funahashi H, Angst E, Go VL, et al. Expression analysis of the prostaglandin E2 production pathway in human pancreatic cancers. Pancreas. 2008; 37:121–7. [PubMed: 18665070]
8. Ito H, Duxbury M, Benoit E, Clancy TE, Zinner MJ, Ashley SW, et al. Prostaglandin E2 enhances pancreatic cancer invasiveness through an Ets-1-dependent induction of matrix metalloproteinase-2. Cancer Res. 2004; 64:7439–46. [PubMed: 15492268]
9. Koshiba T, Hosotani R, Miyamoto Y, Wada M, Lee JU, Fujimoto K, et al. Immunohistochemical analysis of cyclooxygenase-2 expression in pancreatic tumors. Int J Pancreatol. 1999; 26:69–76. [PubMed: 10597402]
10. Okami J, Yamamoto H, Fujiwara Y, Tsujie M, Kondo M, Noura S, et al. Overexpression of cyclooxygenase-2 in carcinoma of the pancreas. Clin Cancer Res. 1999; 5:2018–24. [PubMed: 10473081]
11. Gately S. The contributions of cyclooxygenase-2 to tumor angiogenesis. Cancer Metastasis Rev. 2000; 19:19–27. [PubMed: 11191059]
12. Merati K, said Siadaty M, Andea A, Sarkar F, Ben-Josef E, Mohammad R, et al. Expression of inflammatory modulator COX-2 in pancreatic ductal adenocarcinoma and its relationship to pathologic and clinical parameters. Am J Clin Oncol. 2001; 24:447–52. [PubMed: 11586094]
13. Tucker ON, Dannenberg AJ, Yang EK, Fahey TJ 3rd. Bile acids induce cyclooxygenase-2 expression in human pancreatic cancer cell lines. Carcinogenesis. 2004; 25:419–23. [PubMed: 14656949]
14. Yip-Schneider MT, Barnard DS, Billings SD, Cheng L, Heilman DK, Lin A, et al. Cyclooxygenase-2 expression in human pancreatic adenocarcinomas. Carcinogenesis. 2000; 21:139–46. [PubMed: 10657949]
15. Eibl G, Bruemmer D, Okada Y, Duffy JP, Law RE, Reber HA, et al. PGE (2) is generated by specific COX-2 activity and increases VEGF production in COX-2-expressing human pancreatic cancer cells. Biochem Biophys Res Commun. 2003; 306:887–97. [PubMed: 12821125]
16. Tseng WW, Deganutti A, Chen MN, Saxton RE, Liu CD. Selective cyclooxygenase-2 inhibitor rofecoxib (Vioxx) induces expression of cell cycle arrest genes and slows tumor growth in human pancreatic cancer. J Gastrointest Surg. 2002; 6:838–43. discussion 844. [PubMed: 12504222]
17. Omura N, Griffith M, Vincent A, Li A, Hong SM, Walter K, et al. Cyclooxygenase-deficient pancreatic cancer cells use exogenous sources of prostaglandins. Mol Cancer Res. 2010; 8:821–32. [PubMed: 20530583]
18. Bardeesy N, DePinho RA. Pancreatic cancer biology and genetics. Nat Rev Cancer. 2002; 2:897–909. [PubMed: 12459728]
19. El-Rayes BF, Zalupski MM, Shields AF, Ferris AM, Vaishampayan U, Heilbrun LK, et al. A phase II study of celecoxib, gemcitabine, and cisplatin in advanced pancreatic cancer. Invest New Drugs. 2005; 23:583–90. [PubMed: 16034525]
20. Moore MJ, Goldstein D, Hamm J, Figer A, Hecht JR, Gallinger S, et al. Erlotinib plus gemcitabine compared with gemcitabine alone in patients with advanced pancreatic cancer: a phase III trial of the National Cancer Institute of Canada Clinical Trials Group. J Clin Oncol. 2007; 25:1960–6. [PubMed: 17452677]
21. Choe MS, Zhang X, Shin HJ, Shin DM, Chen ZG. Interaction between epidermal growth factor receptor- and cyclooxygenase 2-mediated pathways and its implications for the chemoprevention of head and neck cancer. Mol Cancer Ther. 2005; 4:1448–55. [PubMed: 16170038]
22. Reckamp K, Gitlitz B, Chen LC, Patel R, Milne G, Syto M, et al. Biomarker-based phase I dose-escalation, pharmacokinetic, and pharmacodynamic study of oral apricoxib in combination with erlotinib in advanced nonsmall cell lung cancer. Cancer. 2011; 117:809–18. [PubMed: 20922800]
23. Lipton A, Campbell-Baird C, Witters L, Harvey H, Ali S. Phase II trial of gemcitabine, irinotecan, and celecoxib in patients with advanced pancreatic cancer. J Clin Gastroenterol. 2010; 44:286–8. [PubMed: 20216081]
24. Gadgeel SM, Ali S, Philip PA, Ahmed F, Wozniak A, Sarkar FH. Response to dual blockade of epidermal growth factor receptor (EGFR) and cycloxygenase-2 in nonsmall cell lung cancer may be dependent on the EGFR mutational status of the tumor. Cancer. 2007; 110:2775–84. [PubMed: 17948911]

25. Zhang X, Chen ZG, Choe MS, Lin Y, Sun SY, Wieand HS, et al. Tumor growth inhibition by simultaneously blocking epidermal growth factor receptor and cyclooxygenase-2 in a xenograft model. Clin Cancer Res. 2005; 11:6261–9. [PubMed: 16144930]
26. Kirane AR, Toombs JE, Larsen JE, Ostapoff KT, Meshaw KR, Zaknoen S, et al. Epithelial-mesenchymal transition increases tumor sensitivity to COX-2 inhibition by apricoxib. Carcinogenesis. 2012
27. Senzaki M, Ishida S, Yada A, Hanai M, Fujiwara K, Inoue S, et al. CS-706, a novel cyclooxygenase-2 selective inhibitor, prolonged the survival of tumor-bearing mice when treated alone or in combination with anti-tumor chemotherapeutic agents. Int J Cancer. 2008; 122:1384–90. [PubMed: 18027868]
28. Ushiyama S, Yamada T, Murakami Y, Kumakura S, Inoue S, Suzuki K, et al. Preclinical pharmacology profile of CS-706, a novel cyclooxygenase-2 selective inhibitor, with potent antinociceptive and anti-inflammatory effects. Eur J Pharmacol. 2008; 578:76–86. [PubMed: 17920584]
29. Schmittgen TD, Livak KJ. Analyzing real-time PCR data by the comparative C(T) method. Nat Protoc. 2008; 3:1101–8. [PubMed: 18546601]
30. Dineen SP, Roland CL, Greer R, Carbon JG, Toombs JE, Gupta P, et al. Smac mimetic increases chemotherapy response and improves survival in mice with pancreatic cancer. Cancer Res. 2010; 70:2852–61. [PubMed: 20332237]
31. Arnold SA, Rivera LB, Miller AF, Carbon JG, Dineen SP, Xie Y, et al. Lack of host SPARC enhances vascular function and tumor spread in an orthotopic murine model of pancreatic carcinoma. Dis Model Mech. 2010; 3:57–72. [PubMed: 20007485]
32. Wang D, Dubois RN. Eicosanoids and cancer. Nat Rev Cancer. 2010; 10:181–93. [PubMed: 20168319]
33. Wang D, Dubois RN. Prostaglandins and cancer. Gut. 2006; 55:115–22. [PubMed: 16118353]
34. de Groot DJ, de Vries EG, Groen HJ, de Jong S. Non-steroidal anti-inflammatory drugs to potentiate chemotherapy effects: from lab to clinic. Crit Rev Oncol Hematol. 2007; 61:52–69. [PubMed: 16945549]
35. Carmeliet P, Jain RK. Principles and mechanisms of vessel normalization for cancer and other angiogenic diseases. Nat Rev Drug Discov. 2011; 10:417–27. [PubMed: 21629292]
36. Ewald B, Sampath D, Plunkett W. H2AX phosphorylation marks gemcitabine-induced stalled replication forks and their collapse upon S-phase checkpoint abrogation. Mol Cancer Ther. 2007; 6:1239–48. [PubMed: 17406032]
37. Xu K, Gao H, Shu HK. Celecoxib can induce vascular endothelial growth factor expression and tumor angiogenesis. Mol Cancer Ther. 2011; 10:138–47. [PubMed: 21220497]
38. Zhu YM, Azahri NS, Yu DC, Woll PJ. Effects of COX-2 inhibition on expression of vascular endothelial growth factor and interleukin-8 in lung cancer cells. BMC Cancer. 2008; 8:218. [PubMed: 18671849]
39. Edelman MJ, Watson D, Wang X, Morrison C, Kratzke RA, Jewell S, et al. Eicosanoid modulation in advanced lung cancer: cyclooxygenase-2 expression is a positive predictive factor for celecoxib + chemotherapy–Cancer and Leukemia Group B Trial 30203. J Clin Oncol. 2008; 26:848–55. [PubMed: 18281656]
40. Ferrari V, Valcamonico F, Amoroso V, Simoncini E, Vassalli L, Marpicati P, et al. Gemcitabine plus celecoxib (GECO) in advanced pancreatic cancer: a phase II trial. Cancer Chemother Pharmacol. 2006; 57:185–90. [PubMed: 16151811]
41. Korpanty G, Carbon JG, Grayburn PA, Fleming JB, Brekken RA. Monitoring response to anticancer therapy by targeting microbubbles to tumor vasculature. Clin Cancer Res. 2007; 13:323–30. [PubMed: 17200371]
42. Katoh H, Hosono K, Ito Y, Suzuki T, Ogawa Y, Kubo H, et al. COX-2 and prostaglandin EP3/EP4 signaling regulate the tumor stromal proangiogenic microenvironment via CXCL12-CXCR4 chemokine systems. Am J Pathol. 2010; 176:1469–83. [PubMed: 20110411]
43. Wang MT, Honn KV, Nie D. Cyclooxygenases, prostanoids, and tumor progression. Cancer Metastasis Rev. 2007; 26:525–34. [PubMed: 17763971]

44. Yao M, Lam EC, Kelly CR, Zhou W, Wolfe MM. Cyclooxygenase-2 selective inhibition with NS-398 suppresses proliferation and invasiveness and delays liver metastasis in colorectal cancer. Br J Cancer. 2004; 90:712–9. [PubMed: 14760389]
45. Jang TJ, Jeon KH, Jung KH. Cyclooxygenase-2 expression is related to the epithelial-to-mesenchymal transition in human colon cancers. Yonsei Med J. 2009; 50:818–24. [PubMed: 20046424]
46. Neil JR, Johnson KM, Nemenoff RA, Schiemann WP. Cox-2 inactivates Smad signaling and enhances EMT stimulated by TGF-beta through a PGE2-dependent mechanisms. Carcinogenesis. 2008; 29:2227–35. [PubMed: 18725385]
47. Handra-Luca A, Hong SM, Walter K, Wolfgang C, Hruban R, Goggins M. Tumour epithelial vimentin expression and outcome of pancreatic ductal adenocarcinomas. Br J Cancer. 2011; 104:1296–302. [PubMed: 21448168]
48. Arumugam T, Ramachandran V, Fournier KF, Wang H, Marquis L, Abbruzzese JL, et al. Epithelial to mesenchymal transition contributes to drug resistance in pancreatic cancer. Cancer Res. 2009; 69:5820–8. [PubMed: 19584296]
49. Tsujii M, DuBois RN. Alterations in cellular adhesion and apoptosis in epithelial cells overexpressing prostaglandin endoperoxide synthase 2. Cell. 1995; 83:493–501. [PubMed: 8521479]
50. Traub P, Perides G, Scherbarth A, Traub U. Tenacious binding of lipids to vimentin during its isolation and purification from Ehrlich ascites tumor cells. FEBS Lett. 1985; 193:217–21. [PubMed: 4065338]

Translational Relevance

Current standard treatment regimens in pancreatic cancer are minimally effective in prolonging overall survival, highlighting the need for novel treatment strategies. The precise function of COX-2 in the tumor microenvironment remains incompletely understood but it has been implicated in tumor angiogenesis and epithelial-to-mesenchymal transition. Apricoxib is a novel COX-2 inhibitor in phase II clinical trials in pancreatic cancer being investigated as a strategy to augment the efficacy of gemcitabine and erlotinib. Here, in preclinical models of pancreatic cancer, apricoxib significantly enhanced the efficacy of gemcitabine plus erlotinib in reducing primary tumor burden and the occurrence of metastases in orthotopic tumor models with elevated COX-2 activity. Strikingly, apricoxib treatment also robustly prevented tumor cells from adopting a mesenchymal phenotype *in vivo*, regardless of COX-2 expression levels by the primary tumor. Enhancing an epithelial phenotype via COX-2 inhibition may improve efficacy of chemotherapy.

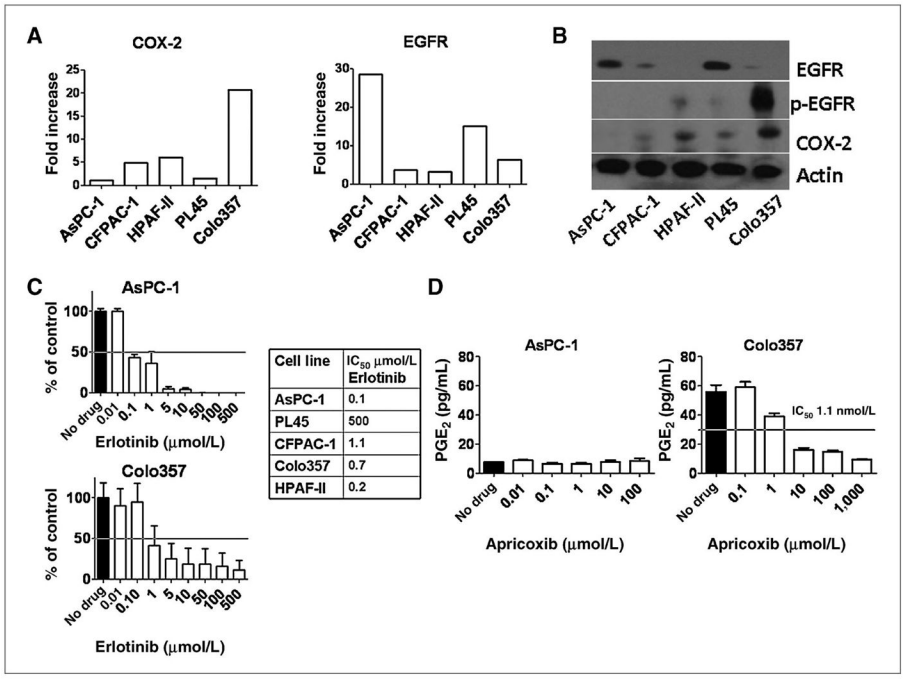

Figure 1.

Baseline expression and functional activity of EGFR and COX-2 in human pancreatic cancer cell lines. A, RNA was harvested from human pancreatic cancer cell lines and evaluated by qPCR for expression of COX-2 and EGFR; levels were normalized to β-actin internal loading control. B, the expression of EGFR, p-EGFR at tyr1068, and COX-2 was determined by Western blot analysis. Expression of β-actin was used as a loading control. C, the IC_{50} of erlotinib for inhibition of phosphorylation of EGFR after stimulation with 10 ng/mL EGF was determined by ELISA. D, PGE_2 levels in conditioned media measured by ELISA after 24-hour incubation with apricoxib.

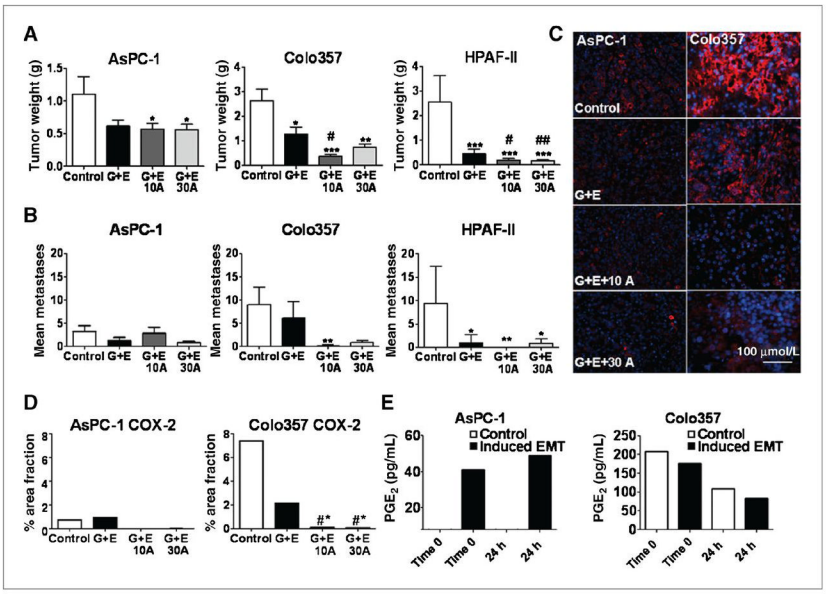

Figure 2.

COX-2 inhibition results in decreased primary tumor growth and metastatic burden. A and B, AsPC-1 (n = 6–8 animals per group), Colo357 (n = 7–8 animals per group), and HPAF-II (n = 7–10 animals per group) human pancreatic cancer cells (1×10^6) were injected orthotopically into the pancreas of SCID mice. Treatment began when established tumor was visible by ultrasound (~ 10 mm^3) and consisted of control (vehicle alone, delivered i.p.), standard therapy of gemcitabine 25 mg/kg twice weekly plus erlotinib 100 µg daily (G + E), or standard therapy plus apricoxib at 10 mg/kg (10A) or 30 mg/kg (30A) daily and continued for 3 or 7 weeks (HPAF-II tumor bearing mice only). Upon sacrifice mean tumor weight (A) and metastatic burden (B) were compared. C and D, paraffin-embedded tumor sections were analyzed for COX-2 expression by immunofluorescence. Data are displayed as mean ± SEM and represent 5 images per tumor with all tumors evaluated. *, $P < 0.05$ vs. control, $^\#$, $P < 0.05$ vs. G + E. Representative images (COX-2, red; DAPI, blue) are shown. Total magnification, 200×; scale bar, 100 µmol/L (C). E, AsPC-1 and Colo357 cells were plated either under normal conditions or under conditions of forced EMT. PGE_2 levels were measured by ELISA in conditioned media at baseline and 24 hours after one time apricoxib dosing at 0.5 µmol/L.

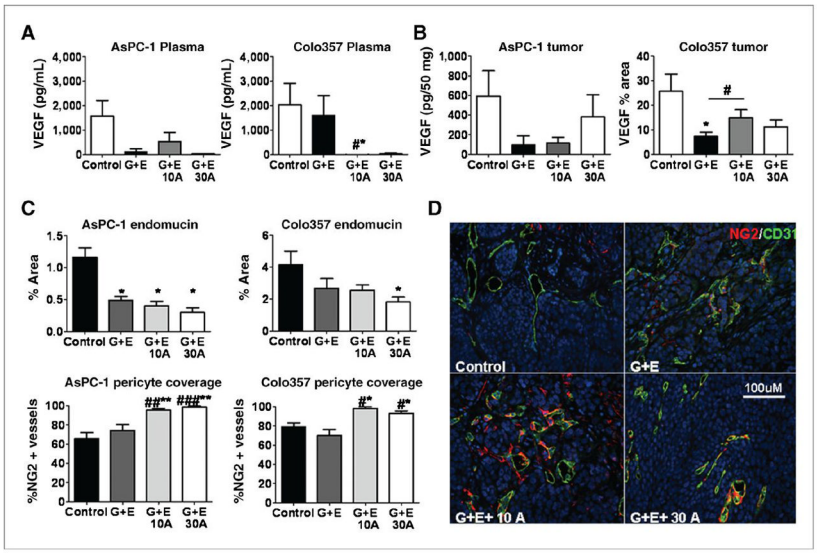

Figure 3.

COX-2 inhibition does not alter intratumoral levels of VEGF or microvessel density but facilitates vascular normalization. A and B, levels of human VEGF in plasma (A) and tumors (B) collected at time of sacrifice were determined by ELISA or immunofluorescence. Mean plasma levels of VEGF are expressed as pg/mL ± SEM and were assayed in triplicate from each animal under study. The level of VEGF in tumor tissue was determined by ELISA (AsPC-1, pg/50 μg protein) or immunofluorescence (Colo357, % area fraction); the mean ± SEM are displayed. C and D, paraffin-embedded sections of AsPC-1 and Colo357 tumors were analyzed by immunofluorescence for endomucin, CD31, and NG2 expression. C, data are displayed as mean ± SEM and represent 5 images per tumor with 5 tumors per group evaluated. D, representative images of CD31 (green) and NG2 (red) are shown for Colo357 tumors. Total magnification, 200×; scale bar, 100 μmol/L. Images were analyzed using Elements software. *, $P < 0.05$, **, $P < 0.01$ vs. control, $^{\#}$, $P < 0.05$, $^{\#\#}$, $P < 0.005$, $^{\#}$, $P < 0.0005$ vs. G + E by 1-way ANOVA.

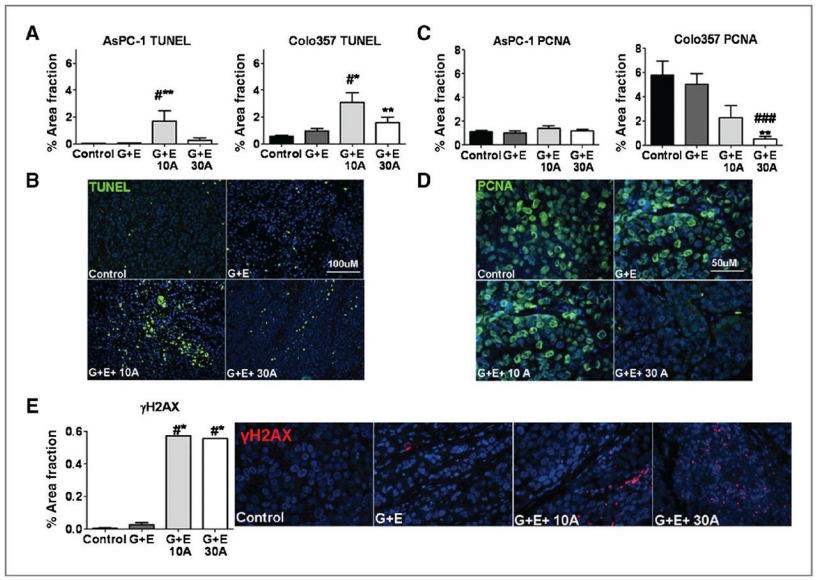

Figure 4.

COX-2 inhibition enhances therapy-induced effects on cell survival and proliferation in pancreatic cancer xenografts. A, apoptosis was evaluated through TUNEL analysis in sections of AsPC-1 and Colo357 tumors. Data are displayed as mean% area fraction ± SEM and represent 5 images per tumor with 5 tumors per group evaluated. B, representative images of TUNEL (green) reactivity in Colo357 tumors are shown. Total magnification, 200×; scale bar, 100 μmol/L. C, paraffin-embedded sections of AsPC-1 and Colo357 tumors were analyzed for cell proliferation (PCNA) by immunofluorescence. Data are displayed as mean% area fraction ± SEM and represent 5 images per tumor with 5 tumors per group evaluated. D, representative images of PCNA (green) immunofluorescence in sections of Colo357 tumors are displayed. Total magnification, 400×; scale bar, 50 μmol/L. E, Colo357 tumors were analyzed for H2AX by immunofluorescence. Data are displayed as mean% area fraction and represent 5 images per tumor with 5 tumors per group evaluated; representative images are shown (H2AX, red; DAPI, blue). Total magnification 400×. *, $P < 0.05$, **, $P < 0.005$ vs. control, $^{\#}$, $P < 0.05$, $^{\#\#}$, $P < 0.005$ vs. G + E.

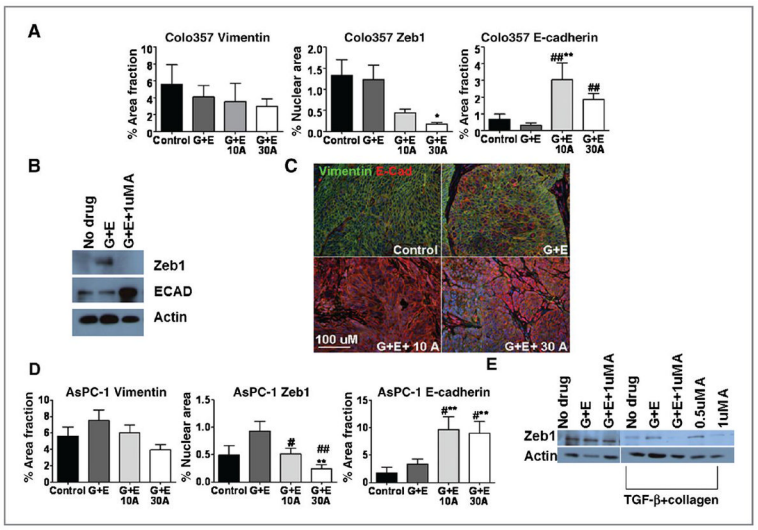

Figure 5.

COX-2 inhibition results in reversal of EMT. A, paraffin-embedded sections of Colo357 tumors were analyzed for E-cadherin, vimentin, and Zeb1 expression by immunofluorescence. Data are displayed as mean% area fraction per high-power field ± SEM and represent 5 images per tumor with 5 tumors per group evaluated. Images were analyzed using Elements software. B, representative images of vimentin (red) and E-cadherin (green) levels in treated Colo357 tumors. Total magnification, ×200; scale bar, 100 μmol/L. C, Colo357 cells *in vitro* were treated with either 100 nmol/L gemcitabine (G) plus 1 μmol/L erlotinib (E) or G + E + 1 μmol/L apricoxib and Zeb1 and E-Cadherin expression was evaluated by Western blot. D, paraffin-embedded sections of AsPC-1 tumors were analyzed for E-cadherin, vimentin, Zeb1 expression by immunofluorescence. E, Western blot analysis of Zeb1 expression by AsPC-1 cells under normal culture conditions or after induction of EMT and treatment with G + E, G + E + apricoxib, or apricoxib single agent. *, $P < 0.05$, **, $P < 0.005$ vs. control, $^{\#}$, $P < 0.05$, $^{\#\#}$, $P < 0.005$, $^{\#\#\#}$, $P < 0.0005$ vs. G + E.

Table 1

Apricoxib enhances *in vitro* sensitivity to gemcitabine

				Gemcitabine, nmol/L				
Cell line	**Apricoxib, μmol/L**	**Erlotinib, μmol/L**	**Gemcitabine, μmol/L**	**1 μmol/L E**	**0.1 μmol/L A**	**1 μmol/L A**	**1 μmol/L A/E**	**Fold change**
ASPC-1	70 (16)	375 (15)	2,000 (0)	1,630 (319)	2,000 (0)	830 (210)	537 (200)	−3.7
Colo357	30 (14)	57 (10)	158 (51)	92 (7)	116 (31)	98 (16)	52 (8)	−2.9
HPAF-II	80 (1)	400 (0)	2,000 (0)	172 (32)	2,000 (0)	400 (23)	13 (2)	−13.2
CFPAC-1	19 (1)	4.3 (1.3)	2.7 (1)	ND	2.1 (0.1)	2 (0.3)	0.72 (0.5)	−3.75
PL45	26 (15)	400 (0)	12.8 (6)	ND	9.6 (1)	9.1 (0.5)	7 (0.6)	−1.8
Su.86.86	77 (8)	400 (0)	2,000 (0)	ND	ND	ND	630 (1)	−3.17

NOTE: The mean IC_{50} (SD) for gemcitabine, erlotinib, and apricoxib was determined by MTS assay as single agents or in combination. Means represent a minimum of 3 independent assays with conditions conducted in octuplicate per assay. The fold change in the IC_{50} for gemcitabine in the presence of apricoxib (A) and erlotinib (E) each at 1 μmol/L is displayed. SD = 0 indicates that an IC_{50} value was not achieved and the maximum concentration of drug used is displayed.

Abbreviation: ND, not determined.